DTU Library

Fabrication and characterization of truly 3-D diffuser/nozzle microstructures in silicon

Heschel, Matthias; Müllenborn, Matthias; Bouwstra, Siebe

[Link back to DTU Orbit](#)

Fabrication and Characterization of Truly 3-D Diffuser/Nozzle Microstructures in Silicon

M. Heschel, M. Müllenborn, and S. Bouwstra

Abstract— We present microfabrication and characterization of truly three-dimensional (3-D) diffuser/nozzle structures in silicon. Chemical vapor deposition (CVD), reactive ion etching (RIE), and laser-assisted etching are used to etch flow chambers and diffuser/nozzle elements. The flow behavior of the fabricated elements and the dependence of diffuser/nozzle efficiency on structure geometry has been investigated. The large freedom of 3-D micromachining combined with rapid prototyping allows to characterize and optimize diffuser/nozzle structures. [199]

Index Terms— Diffuser, laser micromachining, micropump, nozzle, 3-D microstructures.

I. INTRODUCTION

SUBSTITUTING particle-sensitive check-valves in micropumps by diffuser/nozzle elements enables the handling of particle-containing fluids. Medical applications, such as handling of cell fluids like blood, become possible.

Diffuser/nozzle structures, applied as flow diodes in a miniaturized pump, were first presented by Stemme *et al.* [1]. A micromachined pump in silicon, using this working principle, was made by Olsson *et al.* [2]. However, in order to achieve reasonable volume flows and efficiencies for low-power consumption, the diffuser/nozzle elements have to be optimized. The design of diffuser/nozzle elements is a very difficult task, since no general diffuser theory exists because of their complicated flow behavior. A large set of variables is involved, which makes an empirical identification of optimal diffuser design costly in terms of time and labor. In general, the volume flow for a given pressure drop is higher in diffuser than in nozzle direction. The magnitude of this difference, and the efficiency of the structure, depend on the ratio of diffuser outlet to inlet cross-sectional area, the taper angle, and the ratio of diffuser length to inlet diameter. If the opening angle is too large, the opposite effect can be observed as reported by Gerlach *et al.* [3]. Then, the volume flow is higher in nozzle than in diffuser direction.

This paper presents a simple theory for the flow behavior and experimental verification. Truly 3-D microstructures are realized using laser micromachining.

II. THEORY

The pressure drop per length for Poiseuille flow can be described by the Hagen–Poiseuille Law

$$\frac{dp}{dx} = \frac{8\mu}{R^2(x)}V(x) = \frac{128\mu}{\pi D^4(x)}\phi \qquad (1)$$

where $V(x)$ is the mean velocity, ϕ is the volume flow, R or D is the radius or diameter (or hydraulic radius or diameter for noncircular cross sections) and μ is the dynamic viscosity of the fluid [4]. Note that the pressure drop changes proportional to the mean velocity in the case of Poiseuille flow. For a diffuser element with the length L and the taper angle 2θ the linear pressure drop due to Poiseuille flow can be written as

$$\Delta p_l = \int_0^L \frac{128\mu\phi}{\pi D^4(x)}dx = \frac{128\mu\phi}{\pi D_0^4}L\frac{1+\eta+\frac{\eta^2}{3}}{(1+\eta)^3} \qquad (2)$$

with $\eta = \frac{2\theta L}{D_0}$ and D_0 the throat diameter. Considering the rounded inlet, the integral is much more complicated and gives for the linear pressure drop due to Poiseuille flow for a diffuser structure as shown in Fig. 1(a):

$$\Delta p_l = \frac{8\mu\phi}{\pi}\left[\frac{16}{D_0^4}L\frac{1+\eta+\frac{\eta^2}{3}}{(1+\eta)^3}\right.$$
$$\left.-\frac{1}{r^3}\left[\frac{6\beta^4+10\beta^2-1}{6\beta^2(\beta^2-1)^3}+\frac{(4\beta^2+1)\mathrm{arctan}h\left[\frac{1+\beta}{\sqrt{1-\beta^2}}\right]}{(1-\beta^2)^{3.5}}\right]\right] \qquad (3)$$

with $\beta = \left(\frac{R_0}{r}+1\right)$ and r the radius of the rounded inlet. If the flow or velocity in diffuser direction is increased beyond a certain value, separation from the wall occurs (involving back flow) as indicated in Fig. 1(a). Gradients in the flow profile increase more than proportional with flow. An additional pressure drop nonlinear with flow has to be added to the friction pressure drop in order to obtain the total pressure drop

$$\Delta p_D = \Delta p_l + K_D\frac{\rho}{2}(V-V_{th})^2 \qquad (4)$$

where ρ means the fluid density, V_{th} is a transition threshold velocity, V is the throat mean velocity, and K_D is the loss coefficient of the diffuser. The second term in (4) covers the losses due to back flows [4].

In nozzle direction, the flow passes without separation from the wall. The fluid leaves the nozzle always forming back flows, which effectively reduces the effective smallest cross section and extends the effective length. This also gives a nonlinear contribution to the pressure drop, see Fig. 1(b). The total pressure drop in nozzle direction can hence be written as

$$\Delta p_N = \Delta p_l + K_N\frac{\rho}{2}V^2 \qquad (5)$$

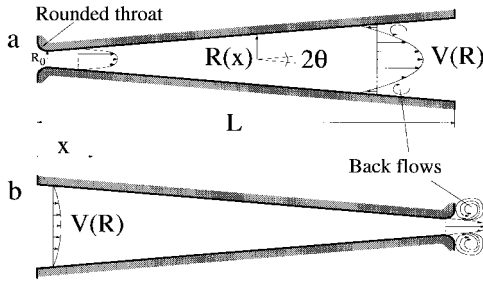where K_N is the loss coefficient of the nozzle.

Fig. 1. Schematic drawing of a diffuser/nozzle element, indicating (a) flow in diffuser direction and (b) flow in nozzle direction, radius $R(x)$, throat radius R_0, taper angle 2θ, structure length L and velocity profiles $V(R)$.
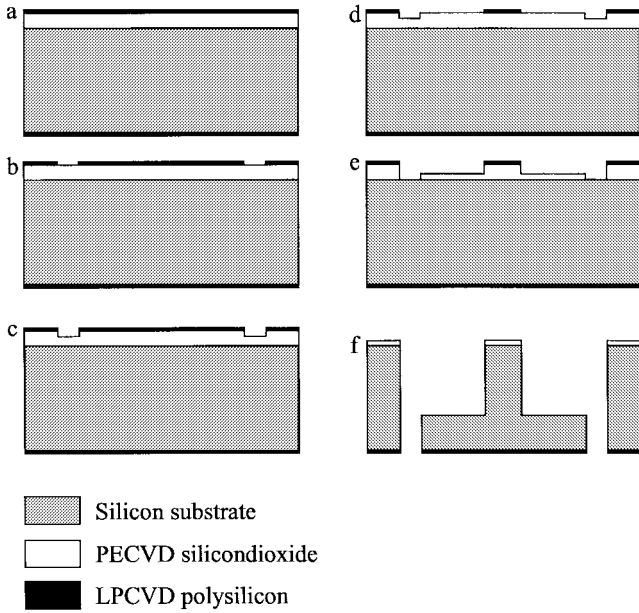

Fig. 2. Process sequence for inlet and outlet chamber fabrication.

TABLE I
DIMENSIONS OF THE FABRICATED DIFFUSER/NOZZLE STRUCTURES. THE VALUES FOR STRUCTURE B ARE THE DEFAULT OR CENTER VALUES. ALL STRUCTURES HAVE A LENGTH OF 1200 μm. THE DEPTH IS EQUAL THE TOP WIDTH, THE BOTTOM WIDTH IS HALF THE TOP WIDTH. ALL OUTLET RIMS ARE SHARP-EDGED

	Taper angle [°]	Throat top width [μm]	Throat shape [μm]
A	6.3	20	round
B	6.3	30	round
C	6.3	40	round
D	4.0	30	round
E	8.0	30	round
F	6.3	30	sharp

RIE in a SF_6/O_2 plasma, as shown in Fig. 2(f). Finally, the remaining SiO_2 is removed in a buffered HF solution.

The chambers are approximately 2×2 mm^2 in area and 200 μm in depth. The via holes have a side length of 400 μm. The first laser-assisted etch step takes approximately 3 s, and the second one takes 80 s using a scan speed of 10 mm/s and a scan width and spot diameter of 5 μm. The SiO_2 etch rate is 0.1 μm/min and the silicon etch rate varied between 2.5 μm/min and 1.9 μm/min, depending on the area of the exposed silicon. SEM photographs of the top view and cross section of a chamber including a via hole are shown in Fig. 3.

Next, diffuser/nozzle structures were realized between each pair of two chambers. The structures have been designed in AutoCAD and directly etched into silicon by laser-assisted etching [6]. Using this technique, truly 3-D micromachining is achievable, resulting in different taper angles, including a controlled taper in the depth direction, structure widths, and inlet and outlet shapes. The etch time varies between 90 min and 150 min for one diffuser/nozzle element, depending on structure dimensions. The scan speed is 5 mm/s and the scan width and the spot diameter 1 μm. The diffuser/nozzle structures have the same taper angle in horizontal and vertical direction. Rounded diffuser inlet rims (when present) have been made in side walls as well as in the bottom. The structures all have a length of 1200 μm and top widths equal to the depths. Their dimensions are presented in Table I. A SEM photograph of a diffuser/nozzle structure between inlet and outlet chambers is shown in Fig. 4. The diffuser inlet is rounded to reduce the entrance pressure loss [7]. The cross-sectional shape is trapeziform, caused by reflection and shadow effects during the laser-assisted etching process. The angle between the silicon surface and the side walls is approximately 76°. Therefore, the bottom width is approximately equal to half of the top width. The roughness of the diffuser/nozzle walls is approximately 1 μm, determined using an optical surface profiler.

Finally, the samples are anodically bonded to 1-mm-thick Pyrex glass to seal them. A plastic holder is glued to the backside to ensure stable connections between inlet and outlet chambers and brass tubes. A complete device containing two diffuser/nozzle structures is shown in Fig. 5.

III. FABRICATION

In order to test the diffuser/nozzle devices, the actual diffuser/nozzle structure, inlet and outlet chambers and via holes have been fabricated according to the process sequence shown in Fig. 2. The diffuser/nozzle structures have been etched by laser-assisted etching, avoiding the need for photo masks and, hence, providing the possibility of rapid prototyping. Moreover, real three-dimensional (3-D) micromachining is possible, including tapered depth as well as rounded corners.

A 350-μm-thick (100) double-side polished silicon wafer is covered at the frontside by a 10-μm-thick plasma enhanced chemical vapor deposited (PECVD) SiO_2, followed by low pressure chemical vapor deposition (LPCVD) of 2 μm of polysilicon [Fig. 2(a)]. Openings corresponding to the desired via holes are etched into the polysilicon applying laser-assisted etching as described by Müllenborn et al. [5] [Fig. 2(b)]. The exposed SiO_2 is then etched 1/3 of the thickness using reactive ion etching (RIE) in a CF_4/CHF_3 plasma [Fig. 2(c)]. A second laser-assisted etch step is applied to define the chamber size, followed by a second SiO_2 etch (RIE) [Fig. 2(d) and (e), respectively]. The resulting stepped SiO_2 structure works as a dynamic mask and is transferred into the bulk silicon via

IV. CHARACTERIZATION

The volume flows are measured by determining weight changes in a given period of time. The used measurement setup is shown in Fig. 6. A pressure difference is applied
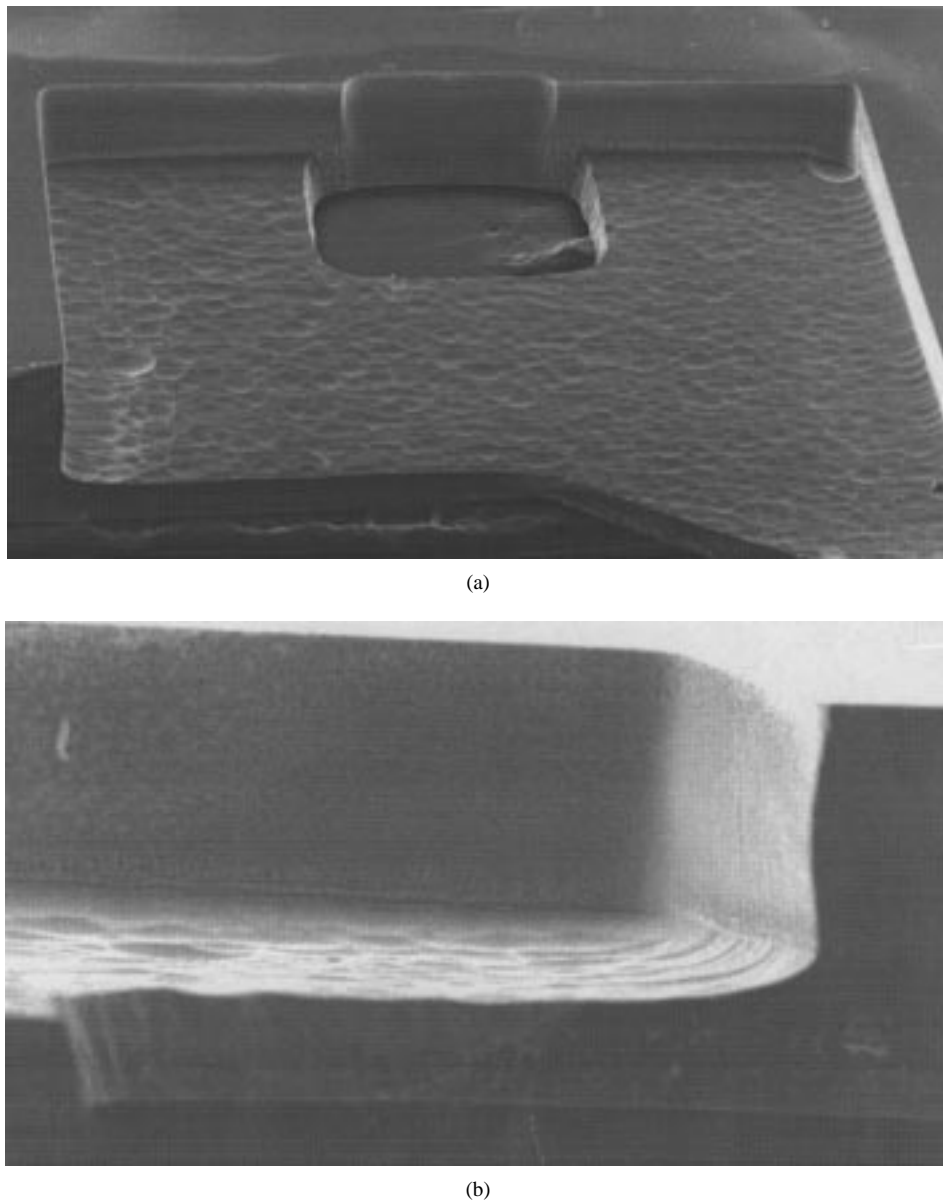
(a)

(b)

Fig. 3.   (a) Top view and (b) cross section of a chamber with a via hole etched using RIE.

to the diffuser/nozzle structure using a pressure controller and calibration device and a pressure chamber filled with water. The weight of the pumped water is measured using a precision balance, with a maximum resolution of 10 μg, which is in the case of water equivalent to 10 nl. The pressure chamber can be moved in the z-direction to keep the pressure chamber and the collecting chamber at the same height level, which is necessary to avoid additional pressure differences. The collecting chamber is covered to prevent evaporation of the pumped water. Rubber tubes ensure a tight connection between all devices. The weight is measured four times and averaged for each pressure difference and converted into the corresponding volume flow using the monitored elapsed time. The sum of all the flow resistances in series with the diffuser/nozzle structures are negligible.

The typical flow behavior of a diffuser/nozzle element is shown in Fig. 7. The experimental values are fitted by applying the following model. The total pressure drop of a diffuser

for low volume flows is only caused by friction effects and increases linearly with an increasing volume flow ϕ. This behavior can be expressed by

$$\Delta p_D = \Delta p_l = R_D \phi_D. \qquad (6)$$

The constant R_D can directly be used to characterize the flow resistance caused by friction. For an increasing diffuser flow a parabolic contribution to the pressure drop is apparent. A threshold flow is observed. Passing this threshold flow, which is different for the different structures, the additional parabolic pressure drop has to be added to the proportional pressure drop. The experimental values for total pressure drop have been fitted using (4). For nozzle flow, no threshold flow is observed. The total pressure drop shows parabolic behavior over the whole pressure range and is fitted applying (5) with $\Delta p_l = R_N \phi_N$. All resulting instead of calculated constants are presented in Table II.
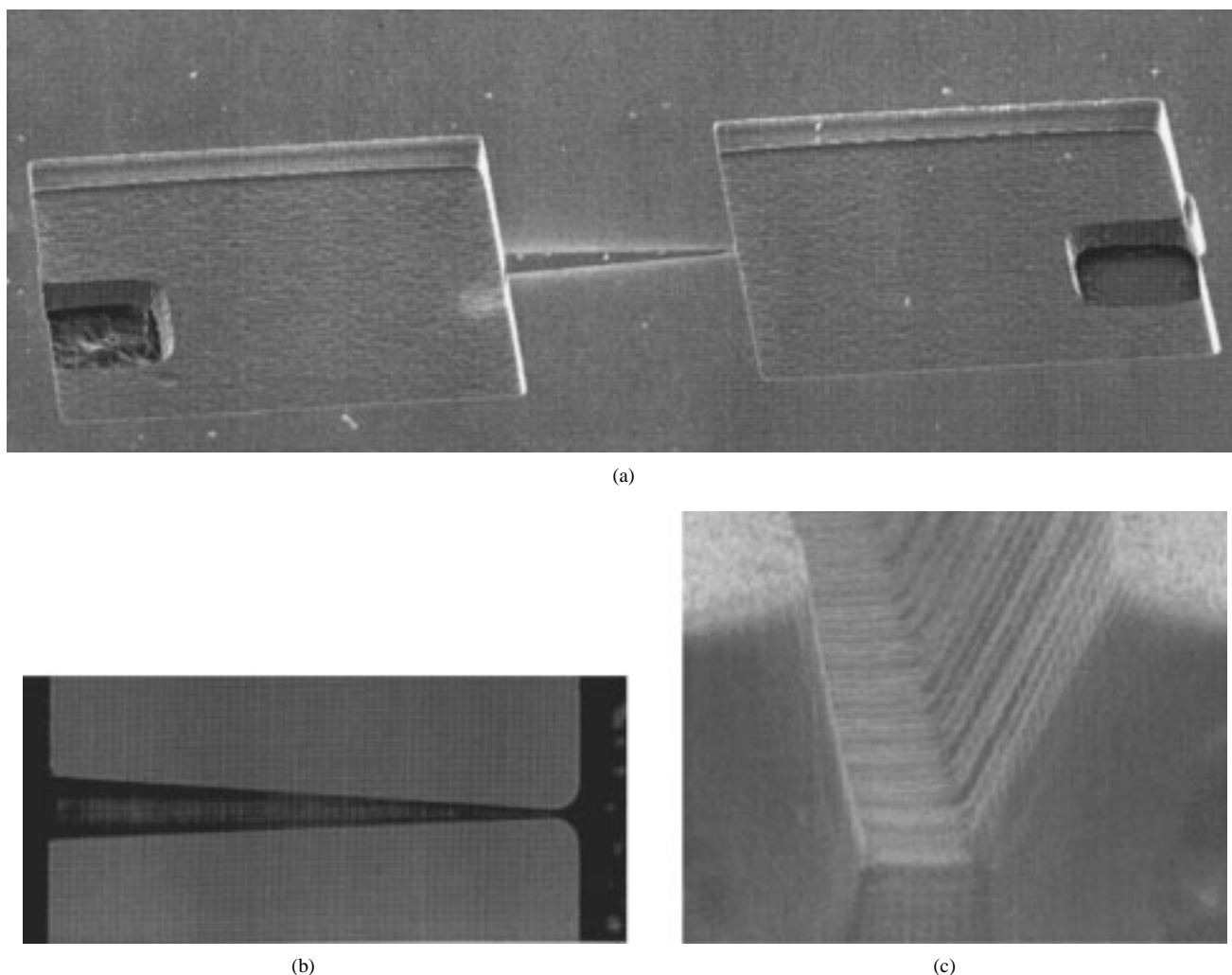
(a)

(b)

(c)

Fig. 4.   (a) Scanning electron micrograph of a diffuser/nozzle structure with inlet and outlet chambers. (b) Photograph of the top view of the structure and (c) close-up of the rounded diffuser inlet.

TABLE II

THE CONSTANTS $R_{D,N}$ DESCRIBE THE LINEAR FLOW RESISTANCE FOR LAMINAR FLOW, THE LOSS COEFFICIENTS K_D AND K_N COVER LOSSES DUE TO BACK FLOWS, AND V_{th} IS THE THRESHOLD VELOCITY FOR TRANSITIONAL FLOW IN DIFFUSER DIRECTION. THE PREDICTED VALUES FOR R_D ARE CALCULATED ACCORDING TO (3), APPLYING THE GEOMETRY FROM FIG. 1(a). THE THRESHOLD VELOCITY IN NOZZLE DIRECTION DOES NOT DEVIATE SIGNIFICANTLY FROM ZERO

	$R_{D,N,predicted}\left[\frac{mbar\cdot min}{\mu l}\right]$	$R_D\left[\frac{mbar\cdot min}{\mu l}\right]$	$R_N\left[\frac{mbar\cdot min}{\mu l}\right]$	K_D	K_N	$V_{th}\left[\frac{m}{s}\right]$
A	3.12	1.57	1.38	0.12	0.23	6.1
B	1.08	1.07	1.01	0.83	1.02	3.2
C	0.44	0.45	0.39	0.85	0.96	2.8
D	1.83	1.32	1.21	0.50	1.08	2.2
E	0.79	0.82	0.78	0.80	0.83	2.8
F	1.37	0.90	0.81	0.83	0.84	3.4

TABLE III

MAXIMUM DIFFUSER/NOZZLE EFFICIENCY IN DEPENDENCE OF NET VOLUME FLOW AND PRESSURE DIFFERENCE

	Max. efficiency [%]	Net volume flow [$\mu l/min$]	Pressure difference [$mbar$]
A	24	360	800
B	26	300	475
C	29	240	130
D	28	400	800
E	22	240	280
F	22	270	350

V. DISCUSSION

The predicted flow resistances calculated according to (3) are confirmed by the experimentally obtained values, except for Structures A, D, and F. The experimental values for nozzle flow are slightly lower than for diffuser flow. The flow resistances $R_{D,N}$ strongly depend on structure dimensions, such as smallest cross-sectional area and taper angle (see Table II). The flow resistances increase with a decreasing cross-sectional area and a decreasing taper angle. The diffuser threshold flow velocity is a weak function of geometry and increases with a decreasing cross-sectional area. For different values of taper angle, a maximum threshold flow is observed for $2\theta = 6.3°$.

The loss coefficients K_D and K_N are weak functions of dimensions, although it does not turn out from structures A and D. The nozzle loss coefficients are slightly higher than the diffuser loss coefficients. Combined with the presence of a threshold velocity in diffuser direction, the pressure drop in nozzle direction is always higher.

The volume flow difference between diffuser and nozzle direction, divided by the average volume flow at equal differential pressure, can be taken as an efficiency.
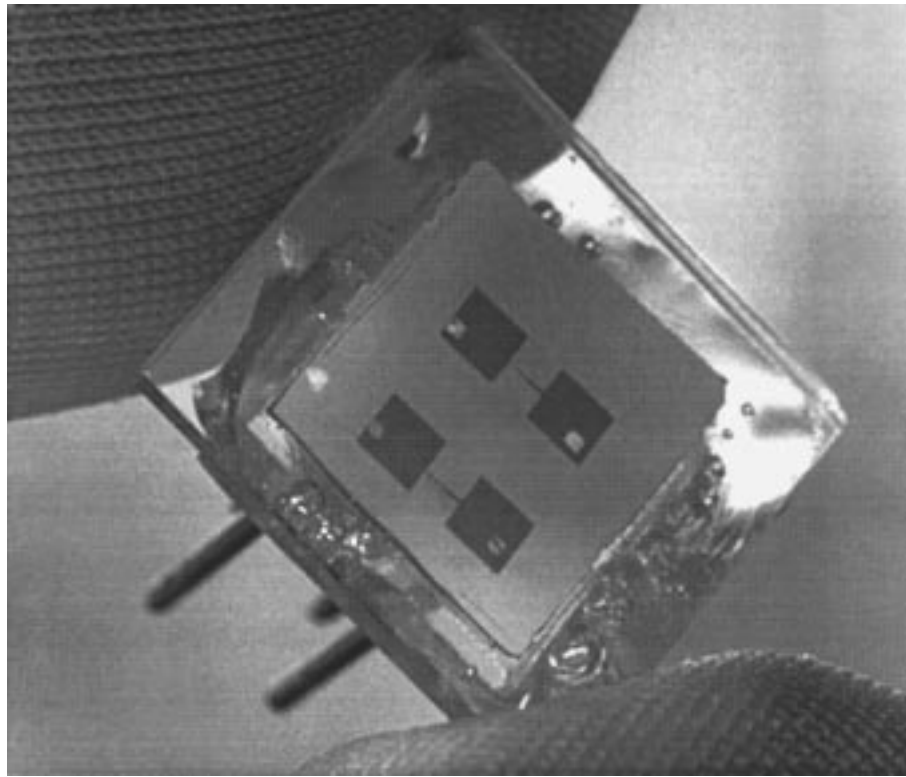
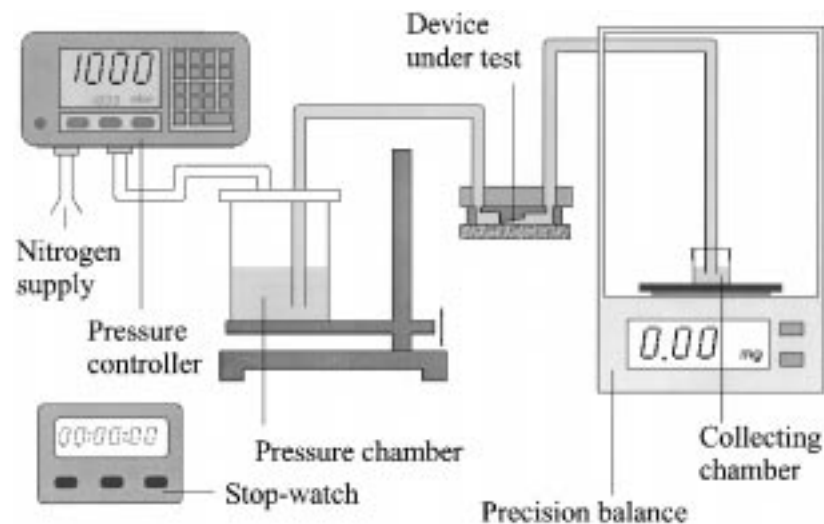Fig. 5. Photograph of a complete device, containing two diffuser/nozzle structures.

Fig. 6. Setup for volume flow measurements.

For different taper angles the efficiency is shown in Fig. 8. The curves are drawn using the best fits from the previous section. The efficiency is zero at zero volume flow, increasing, reaching a maximum, and dropping slowly. The maximum increases slightly with a decreasing taper angle. Note that this increase in efficiency takes place with an increase in volume flow at which it occurs.

Fig. 9 shows the efficiency versus flow for different throat diameters. The efficiency appears to be a weak function of this parameter. The maxima are almost equal, but occur at different volume flows.

The influence of different diffuser inlet shapes on the efficiency is shown in Fig. 10. A diffuser/nozzle element with a rounded inlet yields higher efficiencies than a sharp-edged one. This difference in efficiency can not be observed for the lower volume flow range: for low flows the flow does not separate from the wall.

The maxima efficiencies have been chosen to characterize the flow behavior in dependence on the structure geometry. Table III shows these efficiencies combined with average volume flow and pressure difference at which they occur.
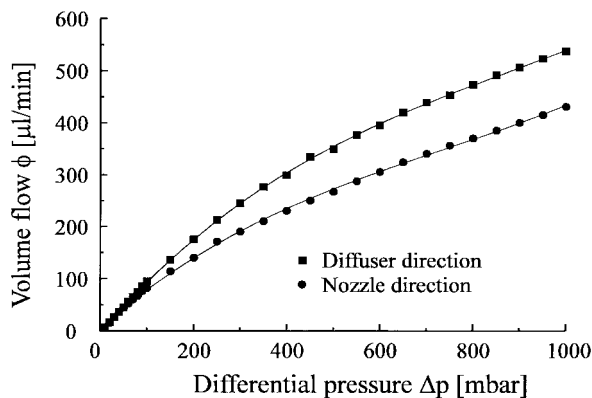
Fig. 7. Diffuser and nozzle volume flow versus applied differential pressure for structure A.
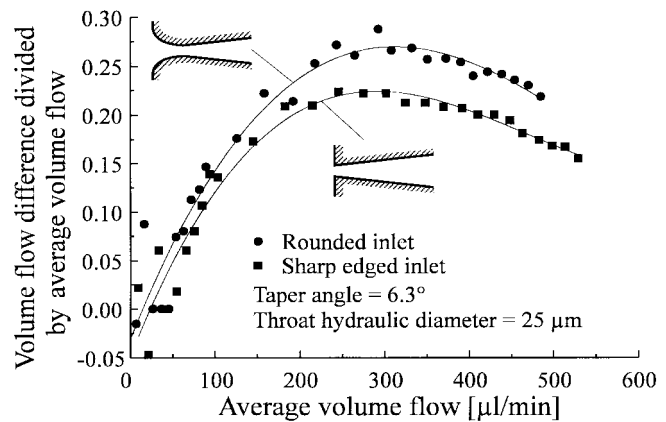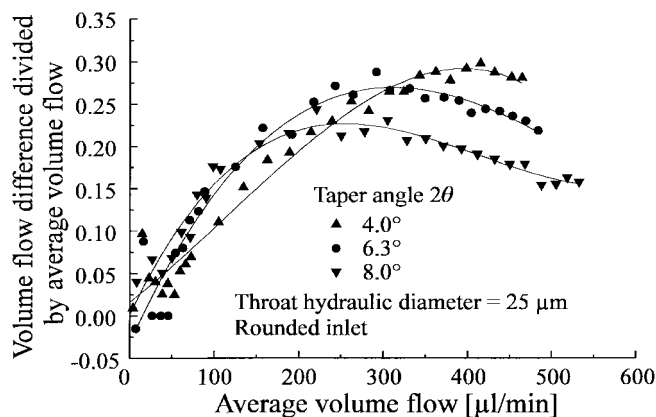

Fig. 8. Difference in volume flow divided by and versus average volume flow at equal differential pressure for different taper angles (structures B, D, and E). The throat cross section and the length are the same for all three structures.
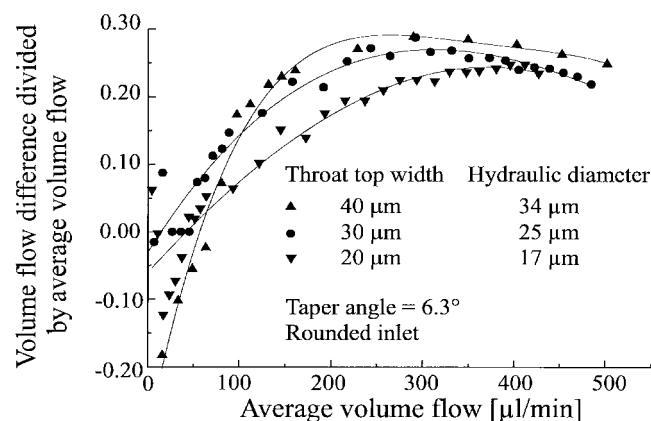

Fig. 9. Difference in volume flow divided by and versus average volume flow at equal differential pressure for different smallest cross-sectional areas (structures A, B, and C). The taper angle and the length are the same for all structures.

Fig. 10. Difference in volume flow divided by and versus average volume flow at equal differential pressure for different throat shapes (structures B and F), everything else being equal.

and laser-assisted etching. Chambers with $90°$ vertical walls and smooth bottoms have been achieved.

Prototypes of diffuser/nozzle elements have been designed and etched into silicon by laser-assisted etching.

The flow behavior of these structures has been investigated and discussed with respect to structure geometries. A model for Poiseuille flow resistance has been developed. The calculated values have been confirmed in most cases by the experimentally obtained values. The loss coefficients for nonlinear behavior have been extracted from volume flow measurements. They show a weak dependence on structure geometry and are slightly higher in nozzle direction than in diffuser direction.

The shape of the structure throat should be rounded in order to improve the flow behavior.

VI. CONCLUSIONS

A process sequence to realize deep inlet and outlet chambers with via holes has been designed, using CVD processes, RIE,

REFERENCES

[1] E. Stemme and G. Stemme, "A novel piezoelectric valve-less fluid pump," in *Dig. Tech. Papers, Transducers'93*, Yokohama, Japan, 1993, p. 110.
[2] A. Olsson, P. Enoksson, E. Stemme, and G. Stemme, "A valve-less planar pump isotropically etched in silicon," *J. Micromech. Microeng.*, vol. 6 pp. 87–91, 1996.
[3] T. Gerlach and H. Wurmus, "Working principle and performance of the dynamic micropump," in *Proc. MEMS'95*, Amsterdam, pp. 221–226, and Creare Inc., Hanover, New Hampshire, 1993.
[4] E. Truckenbrodt, *Strömungsmechanik.* Berlin/Heidelberg, Springer-Verlag, 1968.
[5] M. Müllenborn, M. Heschel, U. D. Larsen, H. Dirac, and S. Bouwstra, "Laser direct etching of silicon on oxide for rapid prototyping," *J. Micromech. Microeng.*, vol. 6, pp. 49–51, 1996.
[6] M. Müllenborn, H. Dirac, J. W. Petersen, and S. Bouwstra, "Fast three-dimensional laser micromachining of silicon for microsystem," *Sensors and Actuators*, vol. A 52, pp. 121–125, 1996.
[7] F. M. White, *Fluid Mechanics.* New York: McGraw-Hill, 1986.

Matthias Heschel received the Master's degree in electrical engineering from the Technical University Chemnitz-Zwickau, Germany. He joined the Microelectronics Center at the Technical University of Denmark in 1994 and is currently working as a Ph.D. student on electrical interconnections and packaging aspects.

Matthias Müllenborn received the Master's degree in physics from the University of Münster, Germany, and the Ph.D. degree in materials science and engineering from the University of California at Los Angeles (UCLA).

His research projects focussed on the optical characterization of III/V materials during his Master's program at the Siemens Research Labs in Münich and on the investigation of heterostructure interfaces at UCLA. He joined the Microelectronics Center at the Technical University of Denmark in 1993, working on high-resolution laser micromachining and nanoscale direct writing. Since 1996, he has been with Microtronic A/S, Denmark, developing micromachined microphones for hearing instrument applications.

Siebe Bouwstra received the Master's degree in mechanical engineering from the University of Twente, The Netherlands. He received the doctorate degree in 1990, from the same university, with his thesis "Resonating Microbridge Mass Flow Sensors."

He joined the Sensors and Actuators Research Unit at the University of Twente in 1984, where he was engaged in industrial and semi-industrial research projects in micromechanics. He was awarded a research fellowship of the Royal Dutch Academy of Science, with which he conducted a collaboration between the MESA Research Institute at the University of Twente and the Center for Integrated Sensors and Circuits at the University of Michigan, Ann Arbor. He joined the Microelectronics Center at the Technical University of Denmark in 1992 as a Research Associate Professor, where he is responsible for the micromechanics research program.